Vol 17 No 9, September 2008
1674-1056/2008/17(09)/3372-06

Chinese Physics B

© 2008 Chin. Phys. Soc.
and IOP Publishing Ltd

Effects of vapour bubbles on acoustic and temperature distributions of therapeutic ultrasound*

Fan Ting-Bo(范庭波), Zhang Dong(章 东)†, Zhang Zhe(张 喆),
Ma Yong(马 勇), and Gong Xiu-Fen(龚秀芬)

Institute of Acoustics, Key Laboratory of Modern Acoustics, Nanjing University, Nanjing 210093, *China*

(Received 25 December 2007; revised manuscript received 14 February 2008)

This paper describes the evolution of vapour bubbles and its effect on nonlinear ultrasound propagation and temperature rise through tissues for therapeutic ultrasound. An acoustic-thermo coupling algorithm incorporating nonlinearity, diffraction, and temperature-dependent tissue properties, is employed to describe nonlinear ultrasound propagation and thermal effect. Results demonstrate that an obvious migration of peak pressure toward transducer surface is observed while the position of peak temperature changes little in liver tissue before the generation of vapour bubbles, and that the boiling region enlarges towards the surface of transducer in axial direction but increases slowly in radial direction after the generation of vapour bubbles.

Keywords: vapour bubbles, ultrasound propagation, temperature rise
PACC: 4335, 8750C

1. Introduction

High intensity focused ultrasound (HIFU) is a noninvasive surgical technique that delivers intense ultrasound energy to a well defined target area of tissue within the body without damage to intervening and surrounding tissues.[1] Thermal and mechanical mechanisms are principally responsible for the therapeutic effects, which is owing to the conversion of ultrasonic energy to heat.[2−4] As a result, the tissue temperature can rapidly increase to values above the protein denaturization temperature (∼43°C), i.e. in the range of 70°C to 100°C. In HIFU therapy, bubbles may come from cavitation (i.e., ultrasound-induced oscillations of microbubbles grown from gaseous nuclei) or boiling due to HIFU induced temperature rise.[5,6] Bubbles are efficient acoustic scatters, they can significantly affect the propagation of acoustic energy to and through the HIFU focus[7] and modify HIFU lesion development, viz. promotion of pre-focal lesions.[8−10] It has been observed that the formation of large bubbles coincides with the appearance of a brightly echogenic region in a B-mode ultrasound image, and triggers visible change of shape lesion growth and migration toward the transducer.[11,12] Additionally, vapour bubbles contribute to the distortion of lesion, and growth of the lesion towards the transducer more than cavitation bubbles.[12] However, up to now, few theoretical models have been built to describe the effect of vapour bubbles on therapeutic ultrasound.

This paper establishes a numerical model to describe the evolution of vapour bubbles, in which the temperature dependant tissue properties is taken into account. The Khokhlov–Zabolotskaya–Kuznetsov (KZK)[13] nonlinear equation is utilized to describe the nonlinear ultrasound propagation in tissues. The Pennes bioheat transfer equation (BHTE)[14] is used to predict the temperature rise in tissues. Moreover, an acoustic-thermo coupling algorithm is employed to incorporate nonlinearity, diffraction, and temperature-dependent tissue properties. Based on the numerical model, the thermo-acoustic lens effect is verified.[15−17] Furthermore, we examine the evolution of bubbles region emanating from the focal zone, and its effect on the acoustic field and temperature distribution. It is expected that the general analysis techniques and the simulation results would help us to know better about the anomalous focused ultrasound phenomena and optimize the therapy treatments.

*Project supported by Program for New Century Excellent Talents in University of China (06-0450) and National Natural Science Foundation of China (Grant No 10474044).
†Corresponding author. E-mail: dzhang@nju.edu.cn

2. Model and method

2.1. Acoustic model

The well known KZK nonlinear equation[13] is used to describe ultrasound propagation in viscous media as the following:

$$\left(4\frac{\partial^2}{\partial\tau\partial\sigma}-\bar{\nabla}_\perp^2-4\alpha r_0\frac{\partial^3}{\partial\tau^3}\right)P=2\frac{1}{\sigma_D}\frac{\partial^2}{\partial\tau^2}P^2, \quad (1)$$

where the normalized variables (ξ,σ) are related to cylindrical coordinate (r,z) with $\xi=r/a$ and $\sigma=z/r_0$, here a is aperture radius of the transmitter and $r_0=\frac{1}{2}ka^2$ is Raleigh distance; k is the wave number; $\tau=\omega(t-z/c_0)$ and $\sigma_{\rm D}=l_{\rm D}/r_0$, here $l_{\rm d}=\rho_0c_0^3/(\beta p_0\omega)$ is the shock formation distance for a planar wave; α is the sound attenuation coefficient and $P=p/p_0$ is the normalized acoustic pressure.

For this study, the numerical solution of Eq.(1) is accomplished using the finite-difference frequency-domain method.[13] The acoustic pressure is decomposed as:

$$P=\sum_{n=1}^{N}(g_n\sin(n\tau)+h_n\cos(n\tau)), \quad (2)$$

where P is the normalized acoustic pressure, g_n and h_n are the nth harmonic coefficients, N is the maximum number of the calculated harmonic order.

2.2. Thermal model

The temperature rise in soft tissue can be modelled by a diffusion type equation. The Pennes BHTE[14] is used to describe the thermal effect of ultrasound in tissue:

$$\frac{\partial T}{\partial t}=\frac{k_{\rm t}}{\rho C_{\rm t}}\nabla^2T-\frac{W_{\rm b}C_{\rm b}}{\rho C_{\rm t}}(T-T_{\rm a})+\frac{Q}{\rho C_{\rm t}}, \quad (3)$$

where T is the temperature in the tissue; $k_{\rm t}$ is the thermal conductivity of the tissue; $C_{\rm t}$ and $C_{\rm b}$ are the heat capacities of the tissue and blood respectively, $W_{\rm b}$ is the perfusion, $T_{\rm a}$ is the ambient temperature (37°C), Q is the heat deposition source term due to the acoustic field. Assuming that the attenuation coefficient α is proportion to f^μ,[18] we obtain the heat source term

$$Q=2\alpha I=\alpha p^2/\rho/c=\alpha_0\sum_{n=1}^{N}p_n^2n^\mu/\rho/c, \quad (4)$$

where α_0 is the attenuation coefficient at the fundamental frequency, Eq.(3) is solved in the cylindrical coordinate by using the finite-difference time-domain method[19] with assumption of the constant flux boundary condition for the edges of the computed zone.

2.3. Temperature dependant tissue properties

Acoustic properties of tissues depend on temperature. HIFU in the focal region raises temperature rapidly enough to the ablation levels and can induce the change of acoustic properties of tissues including sound attenuation, sound velocity and acoustic nonlinearity parameter. The cumulative effect of the variation of acoustic properties will in turn distort the propagation of ultrasonic waves, and affect the distribution of the sound and temperature field.

Figure 1 gives an example of acoustic properties of the porcine liver tissue as a function of temperature, where the temperature dependence of sound speed in liver tissue is described by the mixture law,[20] and the sound attenuation as a function of temperature at 1 MHz is described by Ref.[15].

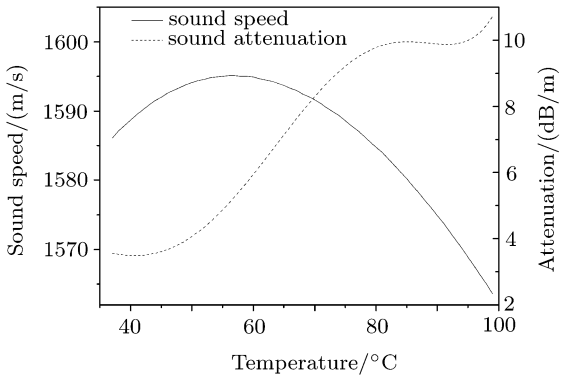


Fig.1. Temperature dependences of sound speed and sound attenuation in liver tissue.

2.4. Acoustic-thermo coupling algorithm

In order to investigate the acoustic-thermal coupling problem, we apply a periodical computation model,[17] which involves the following steps: (1) calculate initial fields of sound and temperature by using Eqs.(1)–(4); (2) update acoustic properties of tissues and then use them as inputs to calculate a new sound field; (3) the sound field driving the heating is in turn affecting the temperature field. Steps 1–3 are repeated in an iterative fashion.

When the tissue temperature in the focal region reaches a boiling point $T_{\rm b}$ (100°C), vapour bubbles

will form, which lead to the sharp decrease of the sound speed and increase of the absorption coefficient. Consequently, the generated vapour bubbles will affect the focused ultrasound field and temperature distribution due to sound reflection and diffraction. Since the volume fraction of bubbles is so small that the bulk modulus is reduced significantly by a factor of 10 or more. In addition, the density of tissue decreases slightly. Consequently, the sound speed $c = \sqrt{K/\rho}$ can be reduced by a factor of 3 or more. In our simulation, for simplicity, the sound speed in boiling/cavitation region is assumed to be zero. It also has been reported that almost all transmitting ultrasound is reflected due to large difference of acoustic impedances between tissue and bubbles.[21] Attenuation coefficient in the boiling regions is nearly infinite, and the energy is absorbed other than transmitted forward into tissue. Consequently, in the computation, the boundary of the bubble region is assumed as absolute soft boundary, viz. the reflecting and transmitting coefficients are set to -1 and 0, respectively. The attenuation coefficient is assumed to be infinite in the bubble region, and in simulation, we set attenuation coefficient as 1000.0 dB/m. In order to study the influence of vapour bubbles, ultrasound field and temperature distribution are computed every 0.1 s after the generation of bubbles.

3. Results and discussions

In this study, a 1 MHz ultrasonic focused transducer (24 mm aperture diameter and 60 mm radius) is utilized as the ultrasound source. The focused ultrasound propagates in the porcine liver tissue, for which the typical parameters are: ρ=1050 kg/m^3, β=6, k_t=0.6 W/(m·K), C_t=3800 J/(kg·K), W_b= 0.5 kg/(m^3·s), and the frequency dependent attenuation coefficient μ=1.266.[22]

The numerical simulation is carried out on an uniform grid with spatial step sizes of 1.7×10^{-4} in axis and 0.01 in radius. The whole computational zone spans a 10 cm (axial)×6 cm (radial) area. The maximum harmonic number is set to N=50.

Figure 2 plots the change of location of the peak pressure over a heating time of 28 s. We select 6 time intervals (0 s, 6 s, 12 s, 18 s, 24 s and 28 s) to illustrate the evolution of axial peak pressures, where the 1st, 2nd and 3rd harmonic components are plotted in Figs.2(a), 2(b) and 2(c) respectively, while the composed sound pressure is plotted in 2(d). It is found that the locations of the harmonic components shift toward the surface of transmitter, and the higher harmonic component corresponds to larger migration. For example, during 28 s ultrasonic heating, the locations of the peak for 1st harmonic component, 2nd

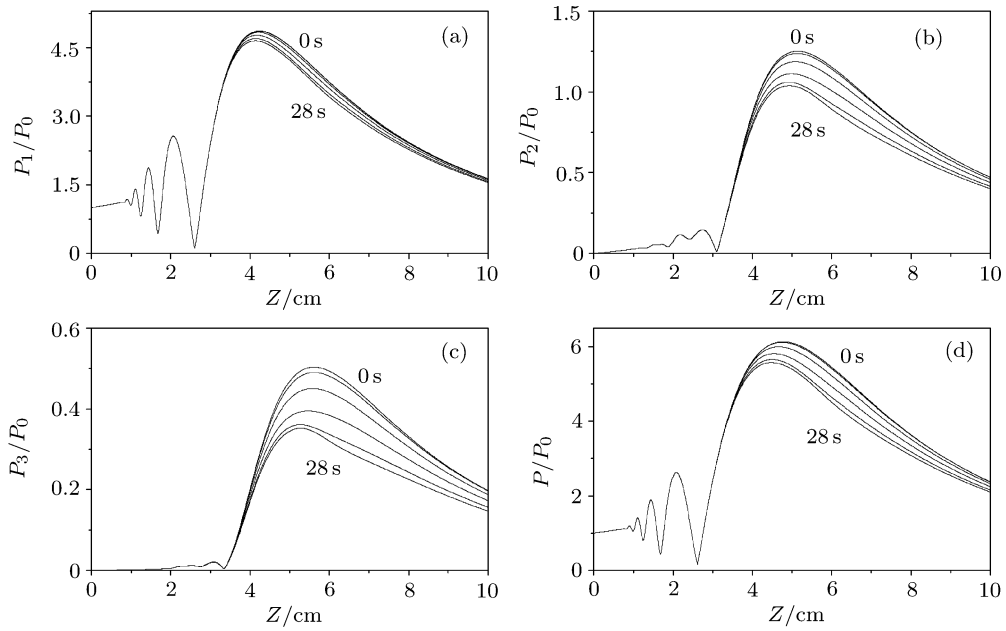


Fig.2. Evolution of axial sound pressures during ultrasonic heating 24 s every 6 s: (a) 1st harmonic component, (b) 2nd harmonic component, (c) 3rd harmonic component and (d) composed pressure.

harmonic component, 3rd harmonic component and composed pressures shift forward about 2.2, 4.2, 6.8 and 6.0 mm respectively. This phenomenon is explained by the thermo-acoustic lens effect due to the temperature dependence of sound speed.[15,16] In addition, the peak pressure amplitudes for the harmonic components decrease during the ultrasonic heating because the absorption coefficient increases with temperature. The higher harmonic component exhibits larger peak amplitude loss, for example, at 28 s the 1st, 2nd and 3rd harmonic components fall about 4.2%, 17.1% and 30.1%, respectively. It is explained by the fact that the absorption coefficient is proportional to f^{u}. Noted that during the initial ultrasound heating, the peak pressure amplitude of the 1st component increases slightly because the temperature changes are not so significant enough to cause the variation of absorption coefficient, while the non-inhomogeneous sound speed distribution makes the peak pressure increase slightly.

Figure 3 simulates the evolution of axial temperature during 2–14 s and 18–28.06 s with a time interval of 4 s. During 2–14 s, the peak temperature increases from 43°C to 67°C. During 18–28.06 s, the peak temperature increases from 77°C to 100°C. It is observed that the location of peak temperature does not shift forward the surface of the transmitter unlike the behaviour of the peak pressure. Noted that the behaviour of the liver tissue is different from that of the fat tissue,[13] in which the peak temperature also shifts forward.

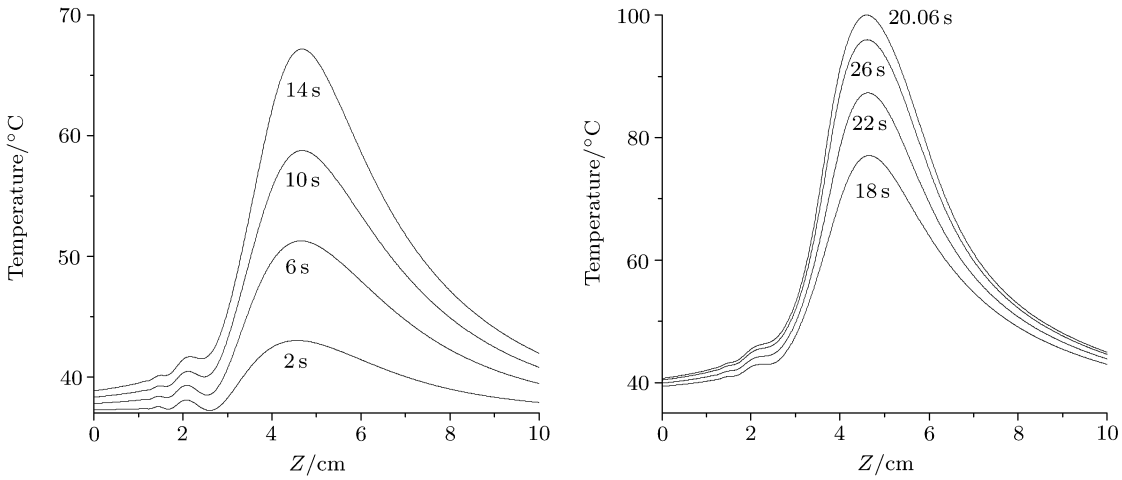


Fig.3. Evolution of axial temperature in 2–14 s and 18–28.06 s.

After 28.06 s ultrasound heating, the temperatures within some axial regions reach 100°C, so vapour bubbles is generated. Once the vapour bubble is generated, the reflecting sound is produced by the reflecting sound waves on the surface of vapour bubble and the heat source term is generated by the linear summation of energy of incident sound field and reflecting sound field.

Figure 4 describes the axial transmitting waves and reflecting wave from 28.0 s to 29.0 s, where Fig.4(a) shows the transmitting wave and Fig.4(b) shows the reflecting wave. We select 4 axial transmitting wave profiles during 28.06 s to 28.96 s to illustrate the change of transmitting waves. In Fig.4(a), at 28.06 s, the acoustic pressure at the interface between tissue and bubble falls down about 45% but not zero because of sound diffraction. As the bubble region increases in axial and radial directions with time, the axial pressure within the bubble region falls down to nearly zero, and decreases sharply beyond the bubble region. In Fig.4(b), the reflecting waves produced by vapour bubbles are attenuated quickly. In the beginning of bubble generation, the region of vapour bubble is very small, and as the vapour bubble region increases, the reflecting sound field is enhanced. Although the reflecting waves attenuate quickly, the reflecting energy near the reflecting surface contributes a lot to the generating of vapour bubble region.

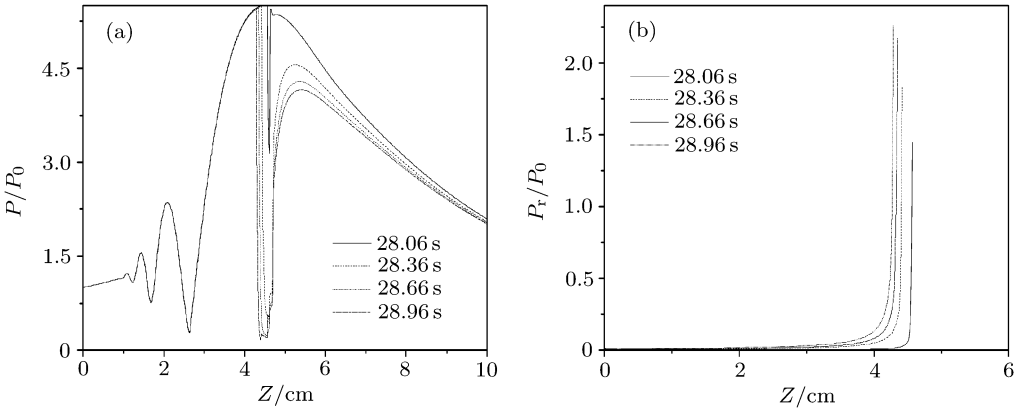


Fig.4. Evolution of axial transmitting wave after bubble generation.

Figure 5 describes the evolution of vapour bubbles region from ultrasonic heating 28 s to 32 s, where Fig.5(a) shows the change of axial locations of bubble region, and Fig.5(b) plots the change of radial length. It is observed from Fig.5(a) that the axial length of boiling region increases with time, and the start point shifts toward transducer surface as a result of reflecting sound wave. However, the end position of the boiling region keeps unchanged between 28 s and 30 s,and after 30 s, the end position shifts forward slightly because the transmitting energy through the boiling region attenuate sharply as seen in Fig.4. On the other hand, the radial change of the boiling region is almost axis-symmetrical, Fig.4(b) plots the change of the maximum radial radius of the bubble region. During the initial 0.3 s after bubble generates (28.06–28.36 s), the maximum radius grows fast from 0.12 to 0.48 mm. From 28.36.0 to 31.0 s, the maximum radius changes slowly from 0.48 to 0.72 mm. From 31 to 31.8 s, the maximal radius almost does not change. The reason is that most energy is focused in the focal region, the temperature beyond the focal region increases slowly. Previously, Chen *et al* experimentally observed the formation process of cavitation bubbles in HIFU.[7] They found that in the initial process, bubble region develops along the axial direction, and that the bubble region shifts forward owing to the reflection of the bubbles. Although the vapour bubbles are different from the cavitation bubble, their developing processes exhibit some similar behaviour.

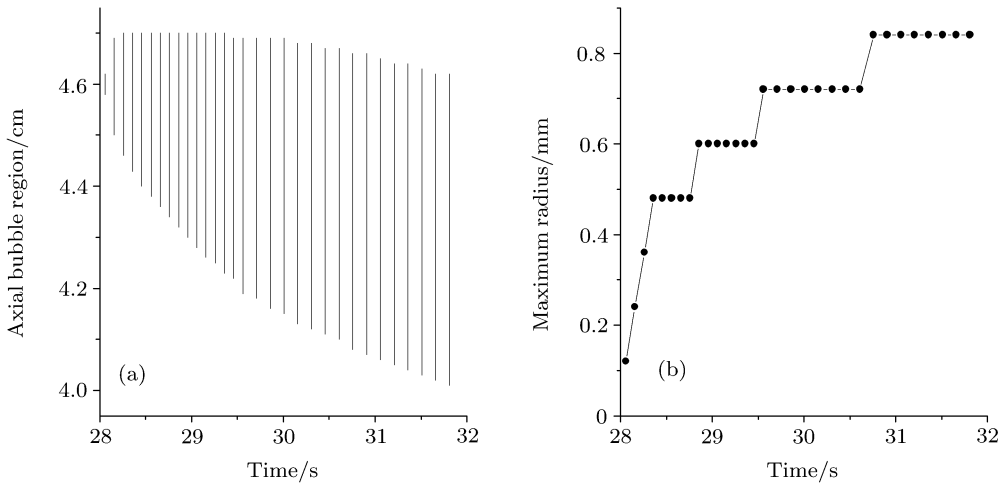


Fig.5. Evolution of axial and radial bubble region from 28.0 s to 32 s.

4. Conclusion

In this paper, we study the influence of vapour bubbles on acoustic field and temperature distribution of therapeutic ultrasound. The nonlinear KZK equation and the Pennes equation are employed to describe nonlinear sound propagation and thermal effect, respectively. Especially, an acoustic-thermo coupling algorithm is used to include the temperature dependences of sound speed and attenuation in tissues. Results demonstrate that 1) the position of peak pressure shifts towards the transducer surface, and the peak pressure amplitude decreases during ultrasonic heating; 2) the position of peak temperature changes little in pure liver tissue; 3) the vapour bubble region enlarges towards the surface of transducer in axial direction, and grows slowly along radial direction about 1.3 s after the generation of bubbles.

References

[1] ter Haar G R 1995 *Ultrasound Med. Biol.* **21** 1089

[2] Malcolm A L and ter Haar G R 1996 *Ultrasound Med. Biol.* **22** 659

[3] Ma Y, Zhang D, Gong X F, Liu X Z, Ma Q Y and Xiu Y Y 2007 *Chin. Phys.* **16** 1009

[4] Qian S Y and Wang H Z 2001 *Acta Phys. Sin.* **50** 501 (in Chinese)

[5] Hynynen K 1991 *Ultrasound Med. Biol.* **17** 157

[6] Holt R G and Roy R A 2001 *Ultrasound Med. Biol.* **27** 1399

[7] Chen H, Li X J, Wan M X and Wang S P 2006 *Acta Acustica* **31** 523

[8] Khokhlova V A, Bailey M R, Reed J A, Cunitz B W, Kaczkowski P J and Crum L A 2006 *J. Acoust. Soc. Am.* **119** 1834

[9] Lizzi F L, Coleman D J, Driller J, Silverman R H, Lucas B and Rosado A 1987 *Proc. the Ultrasonics Symposium* (New York: IEEE)

[10] Lizzi F L 1993 *Eur. Urol.* **23** (Suppl. 1) 23

[11] Fry F J, Sanghvi N T, Foster R S, Bihrle R and Hennige C 1995 *Ultrasound Med. Biol.* **21** 1227

[12] Watkin N A, ter Haar GR and Rivens I 1996 *Ultrasound Med. Biol.* **22** 483

[13] Tjøtta J N, Tjøtta S and Vefring E H 1991 *J. Acoust. Soc. Am.* **89** 1017

[14] Pennes H H 1948 *J. Appl. Physiol.* **1** 93

[15] Hallaj I M, Cleveland R O and Hynynen K 2001 *J. Acoust. Soc. Am.* **109** 2245

[16] Christopher W C and Kullervo H 2002 *Phys. Med. Biol.* **47** 1911

[17] Floch C L, Tanter M and Fink M 1999 *Appl. Phys. Lett.* **74** 3062

[18] Sehgal C M, Brown G M, Bahn R C and Greenleaf J F 1986 *Ultrasound Med. Biol.* **12** 865

[19] Aanonsen S I, Barkve T, Tjotta J N and Tjotta S 1984 *J. Acoust. Soc. Am.* **75** 749

[20] Hallaj I M and Cleveland R O 1999 *ARLO* **1** 7

[21] Wojcik G, Mould J, Lizzi J F, Abboud N, Ostromogilsky M and Vaugham D 1995 *IEEE Ultrasonics Symposium Proceeding* p1617

[22] Meaney P M, Cahill M D and ter Haar G R 2000 *Ultrasound Med. Biol.* **26** 441